Micro- and nanostructured polymer substrates for biomedical applications

Jasmin Althaus[a,b,c,d], Prabitha Urwyler[a,b], Celestino Padeste[b], Roman Heuberger[e], Hans Deyhle[a], Helmut Schift[b], Jens Gobrecht[b,f], Uwe Pieles[c], Dieter Scharnweber[g], Kirsten Peters[d], and Bert Müller*[a]

[a]Biomaterials Science Center, University of Basel, c/o University Hospital, 4031 Basel, Switzerland;
[b]Laboratory for Micro- and Nanotechnology, Paul Scherrer Institut, 5232 Villigen PSI, Switzerland;
[c]Institute of Chemistry and Bioanalytics, University of Applied Sciences and Arts Northwestern Switzerland, 4132 Muttenz, Switzerland;
[d]Department of Cell Biology, University of Rostock, 18057 Rostock., Germany;
[e]RMS Foundation, 2544 Bettlach, Switzerland;
[f]Institutes of Polymer Engineering and of Polymer Nanotechnology, University of Applied Sciences and Arts Northwestern Switzerland, 5210 Windisch, Switzerland;
[g]Max Bergmann Center for Biomaterials, Technical University Dresden, 01069 Dresden, Germany

ABSTRACT

Polymer implants are interesting alternatives to the contemporary load-bearing implants made from metals. Polyetheretherketone (PEEK), a well-established biomaterial for example, is not only iso-elastic to bone but also permits investigating the surrounding soft tissues using magnetic resonance imaging or computed tomography, which is particularly important for cancer patients. The commercially available PEEK bone implants, however, require costly coatings, which restricts their usage. As an alternative to coatings, plasma activation can be applied. The present paper shows the plasma-induced preparation of nanostructures on polymer films and on injection-molded micro-cantilever arrays and the associated chemical modifications of the surface. In vitro cell experiments indicate the suitability of the activation process. In addition, we show that microstructures such as micro-grooves 1 µm deep and 20 µm wide cause cell alignment. The combination of micro-injection molding, simultaneous microstructuring using inserts/bioreplica and plasma treatments permits the preparation of polymer implants with nature-analogue, anisotropic micro- and nano-structures.

Keywords: Injection molding, embossing, PEEK film, plasma treatment, anisotropy, zeta-potential, XPS, mesenchymal stem cells

1. INTRODUCTION

Manufacturing of polymer micrometer-size components with nanostructures on top by mass fabrication is an emerging technology. For example, it is obvious to replace the currently dominating Si- or SiO_2-based MEMS/NEMS components by replicated polymer parts because of substantial cost reductions. These cost reductions, a prerequisite to open further applications, are even more significant, as single usage already required in medicine will become standard in other fields. Several attempts have been made to replace Si micro-cantilevers in sensor systems for biochemical applications by polymer-based microstructures. Either these micro-cantilevers were machined from bulk material [1, 2] or the microstructures were realized in photopolymers using optical lithography [3, 4]. Although it could be shown that polymer cantilevers can be used for sensing, even with substantially higher sensitivity compared to Si, both approaches do have severe drawbacks. The most severe ones are the limited choice of materials and the limited cost advantages expected, since machining of micro-parts and lithography processes are rather expensive. Attempts to apply injection molding in the fabrication of micro-cantilever arrays have been reported [5-7]. The reasons behind might be the precise machining of the molding tool and the control of the molding process for minimizing mechanical stresses in the micro-cantilever arrays.

*bert.mueller@unibas.ch; phone +41 61 265 9660; fax +41 61 265 9699; www.bmc.unibas.ch

Bioinspiration, Biomimetics, and Bioreplication 2012, edited by Akhlesh Lakhtakia, Raúl J. Martín-Palma,
Proc. of SPIE Vol. 8339, 83390Q · © 2012 SPIE · CCC code: 0277-786X/12/$18 · doi: 10.1117/12.915235

The cantilever bending is well known for chemical sensors to identify small amounts of species including DNA. Sensors with cantilevers based on silicon micro-technology have found widespread applications, see e.g. F.M. Battiston [8]. Extreme sensitivity has been reported for detecting mass differences in molecules immobilized on the micro-cantilever's surface. Very recently, polypropylene micro-cantilevers have been introduced to detect bio-molecular interactions [6].

Micro-cantilevers can also be applied to determine the interactions of adherent cells with the underlying substrate. Recently, it has been shown that silicon cantilevers allow measuring the contractile forces of an ensemble of about one hundred fibroblasts [9]. Consequently, the forces of adherent biological cells on any underlying substrate should become accessible. The micro- and nanostructures of the substrate can be intentionally modified to mimic the bony tissue, which exhibits anisotropic features on the micro- and nanometer scale according to the loading direction. In a similar manner cells interact with man-made substrates. A decade ago, it was demonstrated for example that germanium nanopyramids epitaxially grown on Si(100) can drastically reduce the inflammatory reactions [10] and it was postulated that the nanopyramids behave in vitro similar to the apatite crystallites in vivo [11]. This is also the reason why the manufacturers of medical bone implants produce surfaces with a roughness on the micro- and nanometer scale using sandblasting and/or etching procedures. Such procedures, however, do not work equally for polymer implants. Although polymers have many advantages including iso-elasticity and compatibility with magnetic resonance imaging and computed tomography, their usage is still restricted. An appropriate structuring of polymers, which may include plasma treatments [12, 13], will allow the osseointegration of polymer implants and the realization of load-bearing implants with unique properties.

This proceedings communication deals with options to generate micro- and nanostructures on polymer biomaterials, which are supposed to be beneficial for bone implants. Polymer cantilevers, for example, can be straightforwardly micro-structured with a variety of pattern during the injection molding process or using nano-imprint technologies. Such microstructures can reveal directionally defined periodicities to guide and orient adherent cells or even be replicates of natural structures including cortical bone. Further processing, specifically plasma treatment, is necessary to chemically activate the polymer surface and to create nanostructures for improved protein adsorption and related cell behavior. Hence surface morphologies as found in nature (and beyond) are engineered with reasonable effort. Polyetheretherketone (PEEK), a high-performance, FDA-approved polymeric biomaterial is of special interest, since it has similar mechanical properties as human bone and is already used for implants such as housings for pacemakers because of its bio-inertness [14].

2. MATERIAL AND METHODS

2.1 Cantilever manufacture

Arrays of eight polymeric micro-cantilevers were produced using a modular injection molding tool [5, 7]. The molding tool represented in Figure 1 was installed in an Arburg 320 Allrounder (Arburg, Lossburg, Germany) with a maximum clamping force of 600 kN. The mirror unit of the molding tool, a polished steel surface ensured an optically flat and smooth surface. The micro-cantilever array was designed with an outline of $3.5 \times 2.5\ mm^2$ large holder. The eight nominally 45 µm-deep, 500 µm-long and 100 µm-wide micro-cantilever mold cavities were laser ablated. The injection molding process parameters were identical to those published recently [5, 7].

For adding a micro-relief onto the cantilever beam, a thin polycarbonate (PC: Makrofol ID 6-2, Bayer MaterialScience AG, Leverkusen, Germany) film patterned by hot embossing was placed at the mirror side of the molding tool [7]. The mold temperature was low enough to use the polymeric structures for several hundreds replications without degradation of the surface relief. Thus, a simple means to integrate gratings of different sizes and orientations into the micro-cantilever without changing their outlines (see Figure 2) became available.

2.2 Polymers used for injection molding

The polymer materials cyclic olefin copolymer (COC: Topas 8007x10, Topas Advanced Polymers GmbH, Frankfurt-Höchst, Germany), poly-oxymethylene (POM-C: 511P Delrin NC010, DuPont, Le Grand Saconnex, Switzerland), polyvinylidenfluoride (PVDF: Kynar 720, Arkema, Puteaux, France) and polypropylene (PP: Metocene HM648T, LyondellBasell, Bayreuth, Germany) were used for the injection molding experiments presented.

2.3 Polymer films used

For the experiments polyetheretherketone films (PEEK: Series 2000, Victrex Europa GmbH, Hofheim, Germany), polypropylene films (PP: Greiner, Huber, Reinach, Switzerland), polyethylene films (PE: Eppendorf, Huber, Reinach, Switzerland) and polyvinyl alcohol films (PVA: SreenLab, Elmshorn, Germany) were used.

2.4 PEEK sheet embossing

Hot embossing with a HEX03 press (JENOPTIK Mikrotechnik GmbH, Oberkochen, Germany) at a temperature of 160 °C and a pressure of 100 kN served to flatten commercially available amorphous APTIV™ PEEK films with thicknesses of 6, 12, 25 and 50 µm between two polished 4-inch silicon wafers. 20 µm-wide line structures were embossed from a silicon master. Due to processing conditions the PEEK films change from amorphous to partially crystalline phase [15].

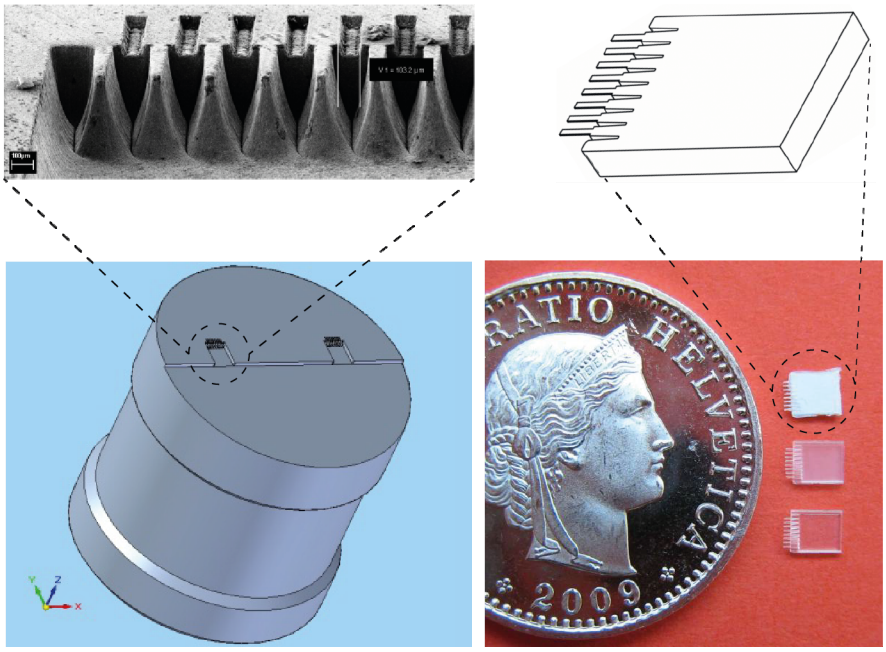

Figure 1. Scheme of the mold insert with two micro-cantilever array cavities each with eight 100 µm-wide micro-cantilevers cavities (left). Three selected injection molded micro-cantilever arrays compared in size to a Swiss coin (21.05 mm in diameter).

2.5 Plasma etching to generate nanostructures on polymer substrates

Oxygen/argon and ammonia plasma treatments (Piccolo system, Plasma Electronic, Neuenburg, Germany) were used to activate the polymer surfaces. First, the specimens were placed at the bottom of the plasma chamber (RF-system, 13.56 MHz). Second, the chamber was evacuated, flushed for a period of 5 min with oxygen/argon (200/100 sccm, 99.5/99.2%, Messer, Lenzburg, Switzerland) or ammonia (200 sccm, 99.98%, Messer, Lenzburg, Switzerland). Third, the system was equilibrated for 5 min with oxygen/argon (20/10 sccm) or ammonia (30 sccm). The plasma treatments with a duration of 5 min using a power of 10 to 200 W resulted in pressures within the chamber of 0.5 to 1.8 Pa and bias voltages from 55 to 400 V.

Since the plasma-activated polymer surfaces are known to exhibit significant changes with time, termed ageing [16], the XPS, zeta potential and presented cell culture experiments were started exactly seven days after the plasma treatments.

2.6 Scanning electron microscopy

The polymer films were coated with a 9 nm-thin Au/Pd film to obtain a conductive surface for scanning electron microscopy (SEM) imaging. During a sputtering time of 30 s (sputter coater Polaron, Thermo VG Scientific, East Grinstead, United Kingdom) with a current of 20 mA under vacuum conditions (6 Pa) the metal film is formed. The

nanostructured substrates were investigated with the field emission scanning electron microscope Supra 40 VP (Carl Zeiss, Jena, Germany) using an acceleration voltage of 10 kV and an InLens detector.

2.7 Zeta-potential measurements

All streaming potential measurements to determine the zeta potential quantitatively were carried out with the Electrokinetic Analyzer (Anton Paar KG, Graz, Austria) unsing silver/silver chloride electrodes and the measuring cell for flat plates as described previously [17]. The temperature, 24 to 28 °C during the experiments, was incorporated into the temperature-dependent viscosity and dielectric constant.

2.8 XPS measurements

X-ray photoelectron spectroscopy (XPS) studies were carried out by means of an Axis Nova photoelectron spectrometer (Kratos Analytical, Manchester, UK). The spectrometer was equipped with a monochromatic Al Kα ($h\nu$ = 1486.6 eV) X-ray source operated at a power of 225 W. The kinetic energy of the photoelectrons was detected using a hemispheric analyzer set to a pass energy of 160 eV for the wide-scan survey spectra and 40 eV for the detailed spectra (full-width-at-half-maximum of $Ag3d_{5/2}$ 1.8 and 0.6 eV, respectively). During the measurements, electrostatic charging of the specimen was overcompensated by means of a low-energy electron source. The CasaXPS software (Version 2.3.15, Casa Software Ltd.) served for peak fittings. The energy scale of the spectra was calibrated against the C1s line peak of aliphatic aromatic carbon at E_b = 284.0 eV. An iterated Shirley background was subtracted from the spectra. Quantitative element compositions were determined from integrated peak areas below the measured curves and corrected by the sensitivity factors provided by Kratos. The residual pressure during the analysis was below $5 \cdot 10^{-6}$ Pa.

2.9 Cell culture experiments

Adipose tissue derived stem cells (ASC) were isolated from liposuction-derived adipose tissue as described previously [18]. Human dermal microvascular endothelial cells (HDMEC) were isolated from juvenile foreskin and cultivated as described in ref. [19]. These in vitro experiments were conducted after approval of the ethics committee (Medical Faculty, University of Rostock) and the full consent of the patients.

In the fourth passage, seeding of ASC was done at 20,000 cells per cm^2. Absence of contaminating monocytes/ macrophages and endothelial cells was confirmed by flow cytometry (FACSCalibur; BD Biosciences AG, Heidelberg, Germany) proving the absence of $CD14^+$/$CD68^+$ (eBioscience, Frankfurt a. M., Germany) and $CD31^+$ (Millipore, Schwalbach, Germany) cells, respectively.

The plasma-treated PEEK films were cut down to fit into a 96-well plates, sterilized with 70% ethanol (LiChrosolv, MERCK, Darmstadt, Germany), washed two times with Dulbecco's phosphate buffer saline (without Ca^{2+} and Mg^{2+}, sterile; PAA Laboratories GmbH, Cölbe, Germany), and incubated with medium for a period of 2 h before cell seeding.

Cell cultivation was carried out under standard conditions, i.e. a temperature of 37 °C and 5% CO_2. Cells were cultured for a period of 48 h on the PEEK substrates and subsequently depicted by the fluorescence stain Calcein-AM (vital stain).

2.10 Live cell staining

Fluorescence staining with calcein AM permitted the visualization of live cells. Here, the cells were incubated in basal medium containing calcein AM (Biomol GmbH, Hamburg, Germany) at 1 µM and incubated for a time period of 15 min at standard conditions, i.e. 37 °C and 5% CO_2 in a humidified atmosphere. Subsequently, the staining solution was exchanged by basal medium and cells were examined under the optical microscope in standard filter-based fluorescence microscopy (Axio Scope.A1 with AxioCam MRc, both Carl Zeiss MicroImaging GmbH, Göttingen, Germany). Calcein excitation and emission maxima are at wavelengths 496 and 516 nm, respectively.

3. RESULTS

3.1 Micro-cantilevers

Additional to micro-cantilever arrays with flat surface given by the polished steel molds, injection molding also permitted the manufacturing of patterned micro-cantilevers [7], i.e. the incorporation of micrometer-size surface topographies on one side of each cantilever. This was achieved by the placement of thermally and mechanically stable, pre-patterned polymer films in the mold. The SEM-images in Figure 2 show a variety of structures obtained for PP micro-cantilevers. The patterns display the high reproduction quality with a precision in the low micrometer range or even below. The rounded microstructures shown in the left image are supposed to be well comparable with cells, whereas the microindentions in the right image will only indirectly interact with cells via the adsorbed proteins.

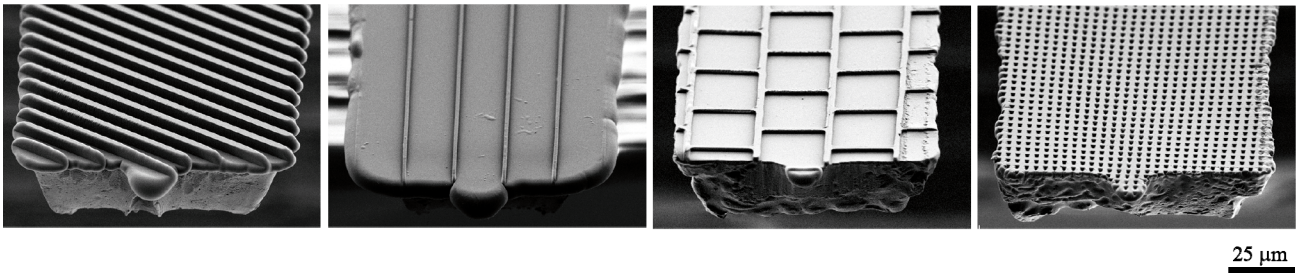

Figure 2. The SEM micrographs of polypropylene micro-cantilevers show the microstructures transferred to the micro-cantilevers during the injection molding process.

3.2 Plasma-treated polymer films

Figure 3 shows four different polymer films that were oxygen plasma treated for a duration of five minutes and a power of 50 W. Oxygen plasma treatments of the originally flat polymer films resulted in nanostructures (three dimensional islands). Although polymer films usually show preferential orientations of the molecules as the result of the casting [15], the plasma treatment yielded only isotropic nanostructures with isotropic distribution, see Figure 3. The larger nanostructures on PMMA, however, showed a ramified morphology.

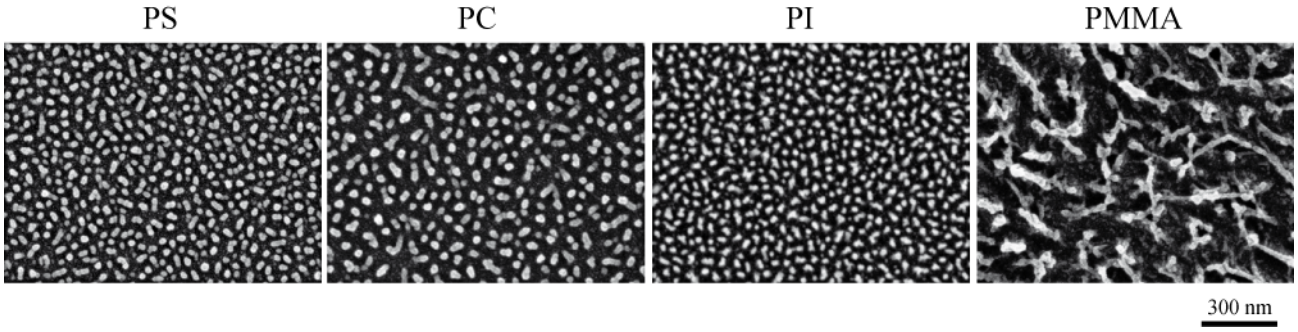

Figure 3. The SEM images of polymer films after oxygen plasma treatment with a power of 50 W show the occurrence of homogeneously distributed nanostructures with material specific size and shape. Whereas polystyrene (PS), polypropylene (PP) and polyimide (PI) give rise to circularly shaped nanostructures polymethyl metacrylate (PMMA) substrates show large ramified nanostructures with an arm width comparable to the diameter of the compact morphologies of the other polymer films investigated.

3.3 Plasma treatment of the micro-cantilevers to generate nanostructures on their surface

Figure 4 shows characteristic surface areas of injection-molded micro-cantilevers prepared from the polymer materials indicated that had been oxygen plasma treated with comparable conditions, i.e. with a power of 50 W and a duration of five minutes each. These SEM images reveal homogenously distributed nanostructures, which are the result of oxygen plasma induced etching. The nanostructure's sizes and density are material dependent and can be further tailored by the choice of the plasma gas composition, the plasma power and the exposure time [12]. The nanostructures on the polypropylene (PP) and polyvinylidene (PVDF) substrates reveal a strong anisotropy. They are elongated and

preferentially oriented. None of the nanostructures observed were compact, although compact shapes are beneficial from an energetic point of view. Therefore, these surface structures represent a metastable configuration.

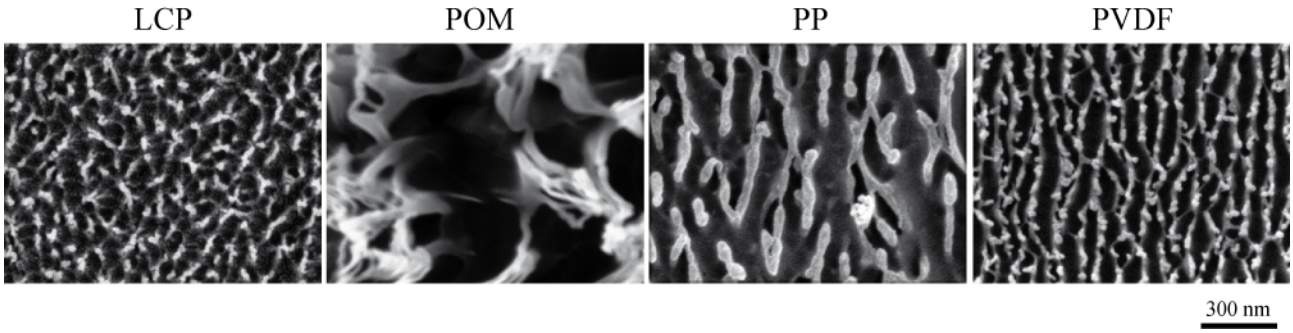

Figure 4. The SEM images of the injection-molded polymers after 50 W oxygen plasma treatment prove the presence of homogeneously distributed nanostructures on the polymer surface. The nanostructures on liquid crystal polymer (LCP) and polyoxymethylene (POM) appear to be isotropic, whereas the ones on polypropylene (PP) and polyvinylidene (PVDF) show an elongated shape with a clear preferential orientation. Size and density of the nanostructures depend on the material selected.

3.4 Injection molding combined with plasma treatment leads to highly anisotropic nanostructures

In injection molded polymer materials, the polymer chains are usually highly oriented as the result of the shear forces occurring during the manufacturing process. Figure 5 shows such anisotropy of injection-molded polyethylene (PE) and polypropylene (PP), as present at the support for the array of the eight micro-cantilevers. For comparison, a polarizer film made of polyvinyl alcohol (PVA) that consists of highly ordered polymer chains is given, cp. ref. [15]. It shows ramified nanostructures but no preferential orientation of the islands. This behavior becomes also clear from images obtained with lower magnification, as shown in the second row of Figure 5.

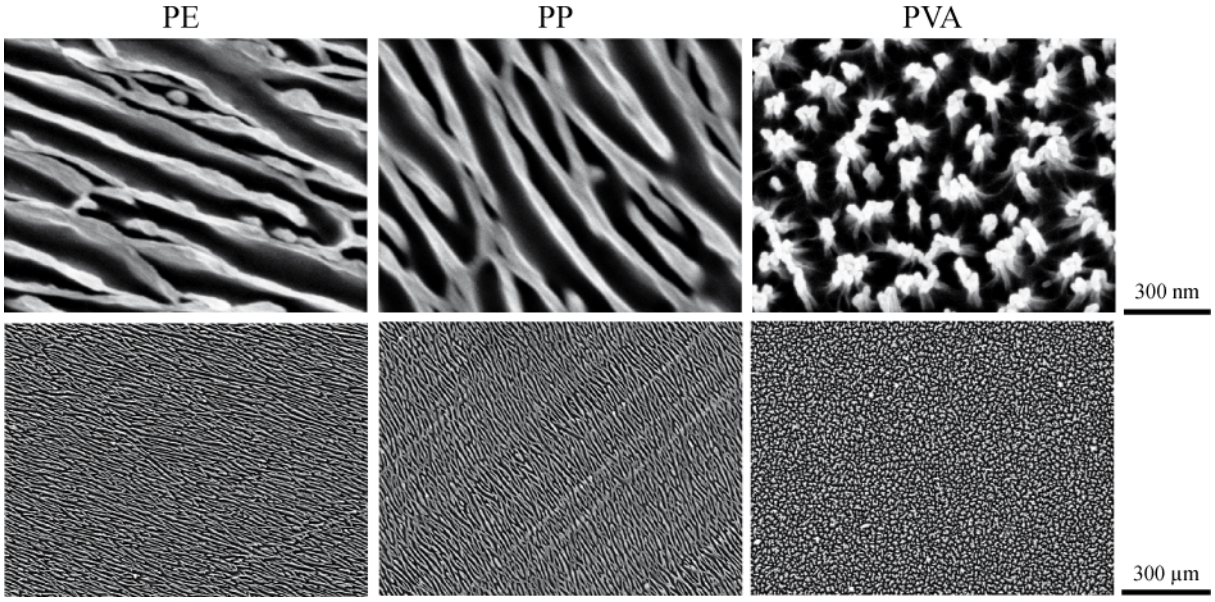

Figure 5. The SEM images of anisotropic polymers treated with 50 W oxygen plasma for five minutes prove that injection molded polyethylene (PE) and polypropylene (PP) exhibit strongly anisotropic nanostructures but the polyvinyl alcohol (PVA) polarizer film that is regularly used for optical purposes does not.

3.5 Comparing oxygen and ammonia plasma treatments of PEEK films

Applying a series of oxygen plasma powers on PEEK films one finds nanostructures of characteristic sizes [12]. For plasma powers up to at least 200 W the size of the pillar-like structures increases with the applied power (see upper part of Figure 6). For ammonia plasma treatments this plasma power dependent phenomenon is also present as shown in the

lower part of Figure 6. Here, the patterning effect is weaker under overall identical conditions (plasma power, duration of treatment and gas flow). This relationship was investigated in detail: A linear dependence between plasma power and roughness and an inverse linear relationship between plasma power and pillar density was demonstrated [12].

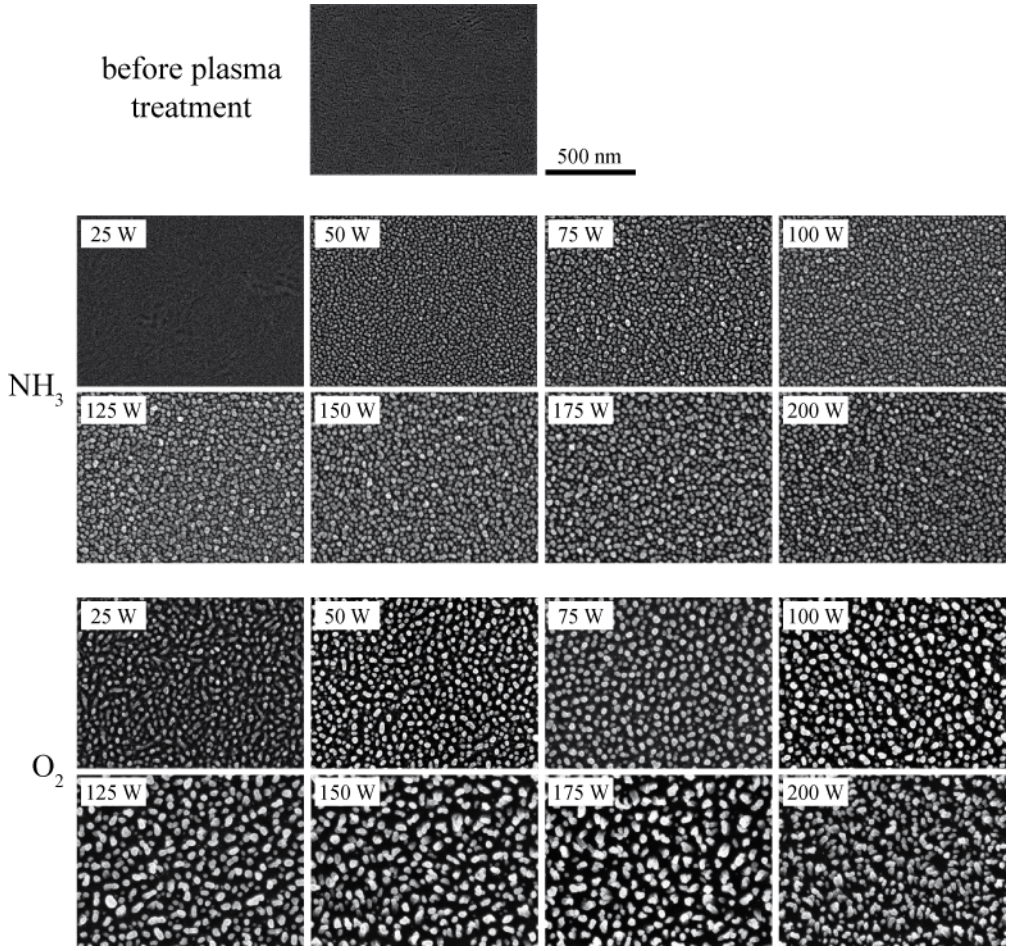

Figure 6. SEM images of oxygen and ammonia plasma treated polyetheretherketone (PEEK) films after applying plasma powers from 25 to 200 W during five minutes. The pillar-like, nanometer-size features increase with plasma power. Ammonia plasma is less abrasive than oxygen plasma.

3.6 Stability of generated nanostructures

In order to investigate the stability of the generated nanostructures on the PEEK films for planned cell studies, washing and sterilization procedures were performed. Figure 7 displays the related SEM images. Neither excessive rinsing with water nor the standard sterilization procedure consisting of a 70% ethanol wash followed by rinsing with phosphate buffered saline and water destroyed the nanostructures. The washing procedures, however, change the size and shape of the pillar-like PEEK nanostructures. The larger nanostructures show a ramified shape, which seems to be the result of aggregated pillars.

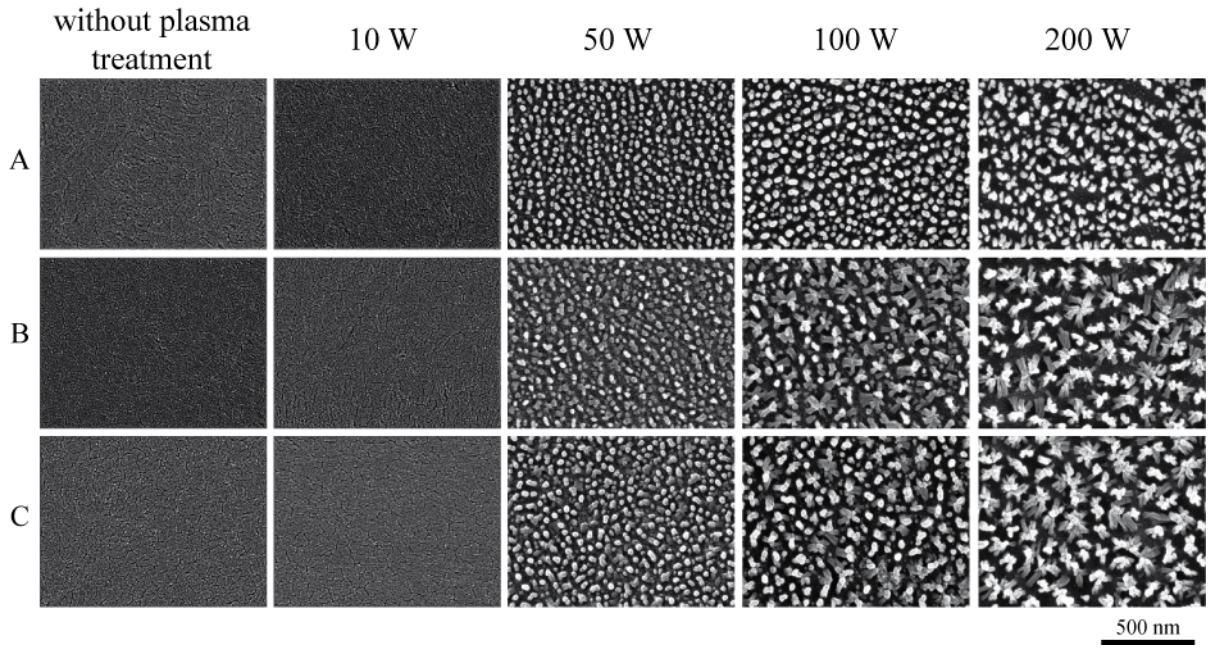

Figure 7. The SEM images of oxygen plasma treated PEEK substrates show (A) the morphology of dry films directly after the plasma treatment, (B) the morphology of the substrates after rinsing with water twice and dried in air, and (C) the morphology of the plasma-treated PEEK substrate after rinsing with 70% ethanol, with PBS twice and four times with water before dried in air.

3.7 Zeta-potential measurements

Plasma-excited oxygen and ammonia are reactive gaseous species that not only etch the PEEK surface and give rise to characteristic nanostructures but also induce a chemical alteration of the PEEK surface. In the field of biomaterials science and engineering such changes are often characterized by zeta-potential measurements that describe the surface charge as a function of the pH. Note surface charges crucially determine the protein adsorption thermodynamics and kinetics. For films, as given in the present case, the zeta-potential is commonly determined by the pH-dependent streaming measurements as shown in the diagram of Figure 8. The pH-value found for a zeta-potential of zero, i.e. at a net charge of zero, corresponds to the iso-electric point of the surface. The original flat PEEK substrate revealed an iso-electric point of 3.9. The oxygen plasma treated films showed a substantial shift towards lower iso-electric points. Ammonia plasma treatments caused a shift of the iso-electric point to slightly more basic pH-values. The ammonia plasma-treated PEEK surface seemed to be less stable than the oxygen plasma-treated surface since the zeta-potential shifted during the equilibration at the beginning of the measurement from higher values towards the values of the untreated PEEK film. The oxygen plasma-treated PEEK films exhibited a constant zeta-potential from the start of the experiment.

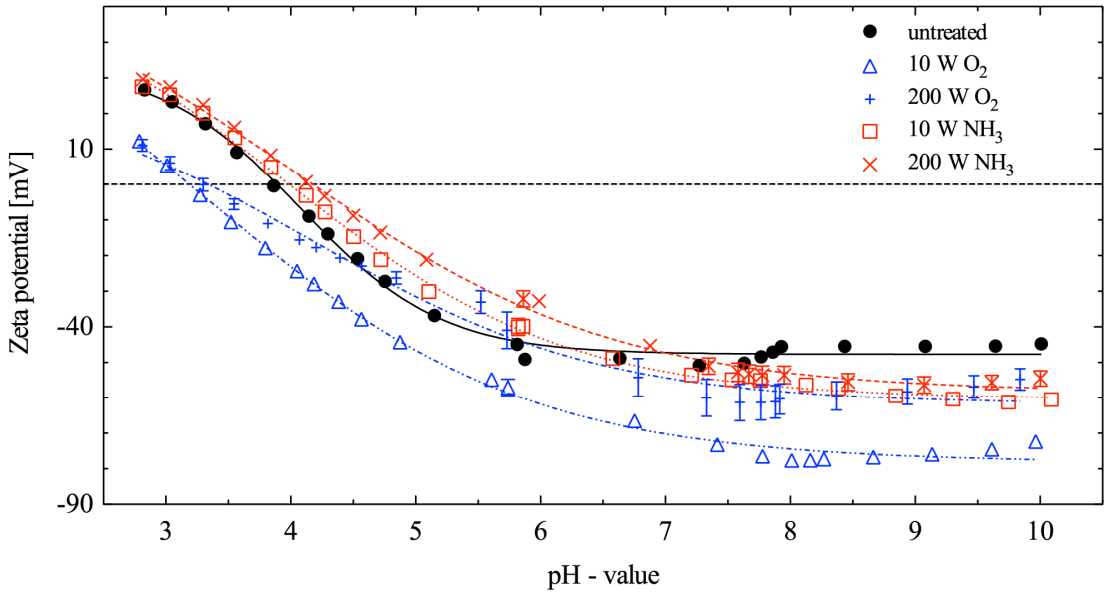

Figure 8. The zeta-potential of oxygen plasma treated PEEK films is shifted to smaller values with respect to the original PEEK film, whereas the ammonia plasma treatment resulted in higher values than the original PEEK substrate.

3.8 Chemical analysis of the plasma treated PEEK films using XPS

To gain more detailed information about the chemical modification of the PEEK film surfaces induced by the plasma treatment, XPS measurements were performed. The summary of the results for the oxygen plasma treated PEEK substrates is displayed in Figure 9. The survey scans in the first column show an increase of oxygen with increasing applied plasma power. Significant amounts of fluorine and aluminum are also present on the plasma treated surfaces, generally increasing with applied plasma power.

The highly intense peak at 284.5 eV of the C1s spectrum corresponds to the aromatic carbon atoms [20]. The peaks of higher binding energy are attributed to the following functional groups: ether bonds (C-O-C, 286.1 eV), keto bonds (C=O, 286.9 eV), carbonyl, ester and carbonate bonds (COOx, CO_3, 288.3 eV) and shake-up satellite bonds from the π-electrons of the aromatic rings [20]. The C1s spectra revealed the formation of C-OOH and carbonate groups upon oxygen plasma treatment, which was previously well documented [16, 21]. A plasma power dependent decrease of the carbonyl groups and the aromatic C-C bonds was caused by the bombardment and associated fragmentation of the surface PEEK molecules. The O1s spectrum of the original PEEK film showed two main peaks for the ether bonds (532.7 eV) and keto bonds (531.3 eV) [20] and a minor peak at higher binding energy due to absorbed water [22]. The differences in peak-shape and the increased intensity in the O1s spectra are assigned to the various oxygen-containing species formed in the plasma process. A minor amount of nitrogen was found on the oxygen plasma treated PEEK surfaces at binding energies of 400 and 402 eV, which can be attributed to aliphatic amine groups (-C-NH2) and charged amine groups, respectively, [23].

Ammonia plasma treatment introduced additional amounts of nitrogen and oxygen on the substrate surface as can be seen in Figure 10. The fitted N1s peaks (at (399.8 eV and 402.1 eV) are assigned to the formation of amine groups, which only a minor amount was charged. Surprisingly the nitrogen content was highest at intermediate plasma power. This is most probably due to increased sputtering of the surface at high plasma power. Sputtering leads removal of formed surfaces species and to the formation of surface radicals which undergo further reactions, e.g. with oxygen and water of the environment when the samples are removed form the plasma chamber. These reactions explain the increased intensity of the O1s signals upon NH_3-plasma treatment and are in line with the additional peaks found in the C1s spectra. Similar to the O_2-plasma-treatment we also found increasing fluorine and aluminum concentrations with increasing plasma power.

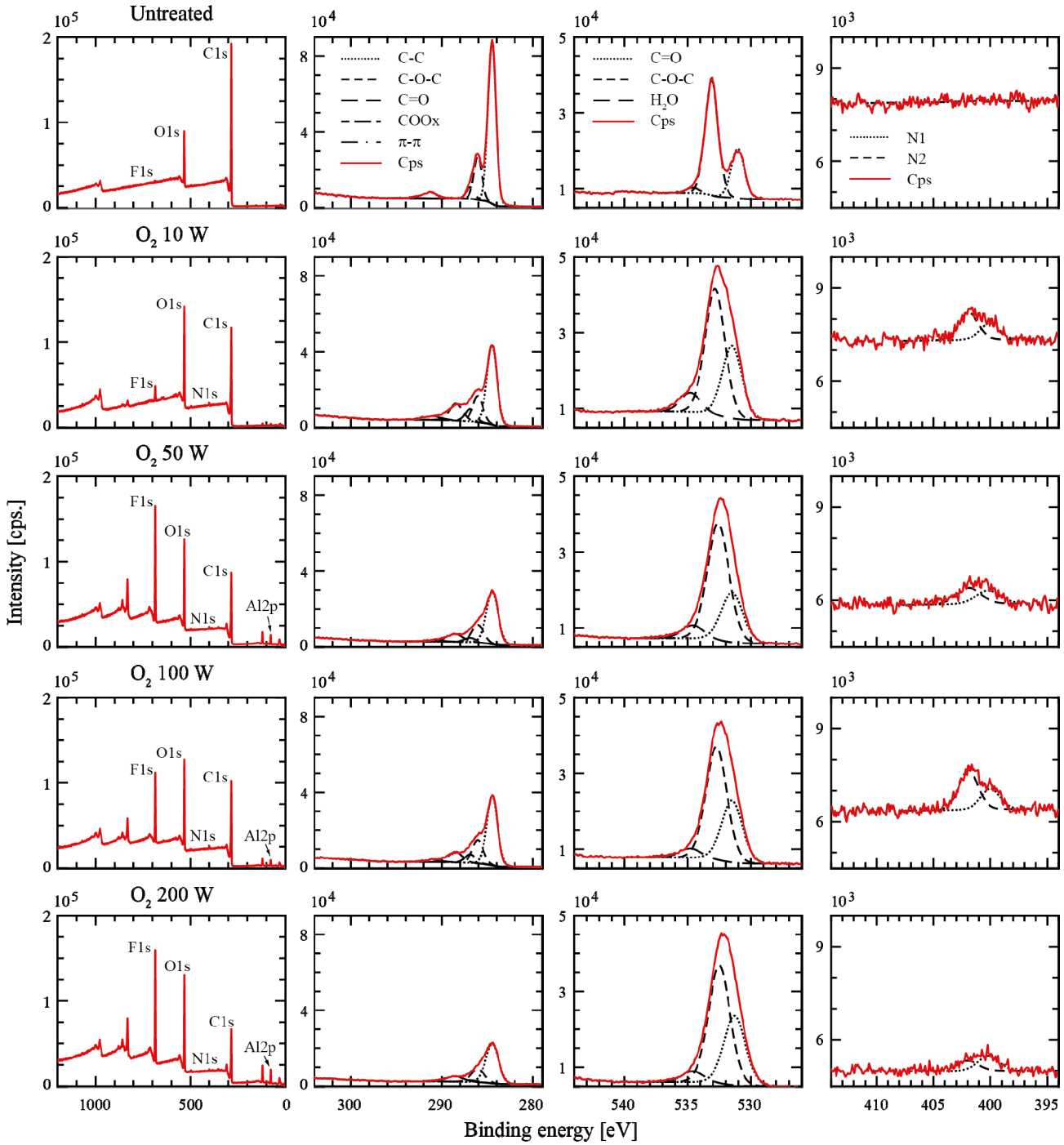

Figure 9. XPS spectra of oxygen plasma treated PEEK films. Survey spectra (first column) and detailed spectra of C1s, O1s and N1s.

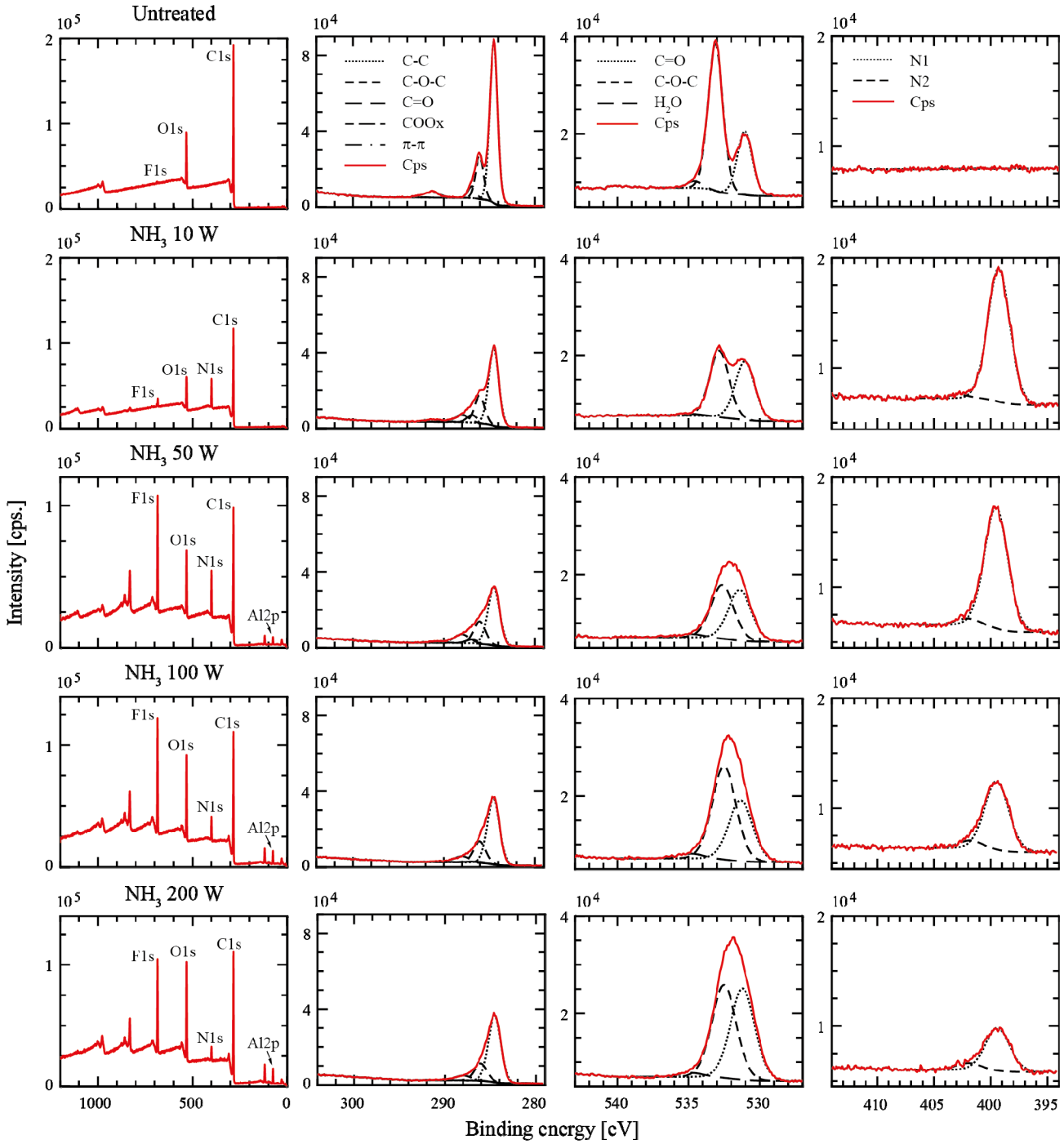

Figure 10. XPS spectra of ammonia plasma treated PEEK films. Survey spectra (first column) and detailed spectra of C1s, O1s and N1s.

3.9 Cell response to plasma-treated PEEK substrates

The initial cell adhesion on the plasma-treated PEEK substrates with two primary cells types, HDMEC (human dermal microvascular endothelial cells) and ASC (adipose tissue derived stem cells), is depicted in Figure 11 by optical micrographs of the stained cells (vital staining). Both cell types did not adhere homogenously on the original, not plasma-treated PEEK substrate but were well spread and grew to confluence after 48 h on the polystyrene control (tissue culture polystyrene – TCPS) and the ammonia plasma-treated PEEK substrates.

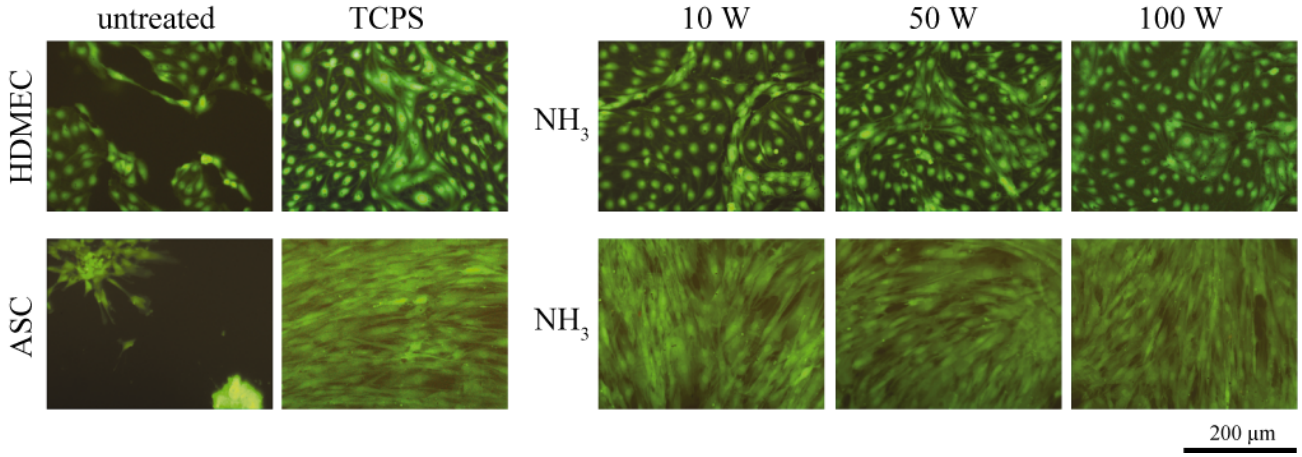

Figure 11. The optical micrographs show adipose tissue derived human mesenchymal stem cells (ASC) and human dermal microvascular endothelial cells (HDMEC) on ammonia plasma-treated PEEK substrates 48 h after seeding. The cells were stained by means of the green fluorescent intracellular calcein-AM vital stain. Both cell types do not homogenously adhere to the untreated PEEK substrate but on the ammonia plasma treated substrates without exception.

Cells are known to react to their underlying substrate on the micrometer and nanometer scale [10, 24, 25]. Therefore, micro-structured PEEK substrates with grooves 1 µm deep and 20 µm wide were fabricated and additionally plasma treated to activate the substrate and to realize the nanometer-size features on top. ASC stretched and aligned parallel to such grooves and displayed an elongated phenotype as clearly verified in Figure 12. The control measurement on TCPS without grooves showed a random orientation of the adherent ASC. The ASC adhered to the original PEEK substrate did not reveal such homogeneous distribution as on the plasma-treated PEEK films. Both oxygen and ammonia plasma treated PEEK substrates allowed homogenous ASC adhesion. Adding a 5 nm-thin titanium film onto the PEEK surfaces always resulted in a homogenously distributed cell layer.

The images taken in the red emission channel are supposed to uncover the dead cells stained by propidium iodide (PI). No dead ASC were found on the substrates. The images, however, allow detecting the micro grooves of the PEEK films because of the strong broadband auto-fluorescence of PEEK [12].

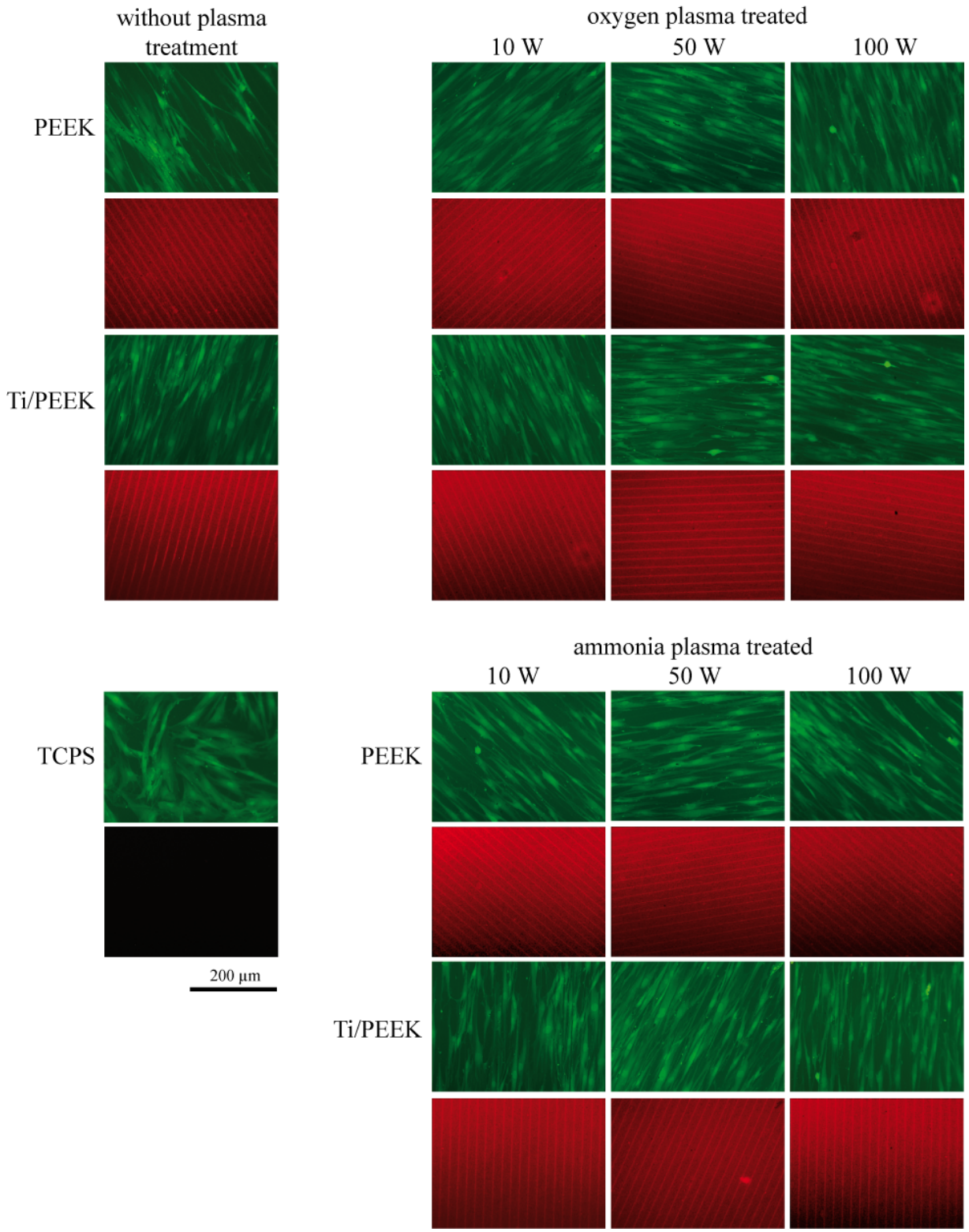

Figure 12. ASC aligned along micro-grooves on oxygen and ammonia plasma treated PEEK substrates 48 h after seeding. Vital cells were stained with calcein-AM. The micro-grooves including their orientation are visible in the red-colored images.

4. DISCUSSION

Improved design of injection molds and optimized processing allow the fabrication of polymer parts with dimensions in the micrometer range, which can be successfully applied as biosensors to detect DNA sequences or nM copper ion concentrations [6]. Such tiny products, however, are not yet medical implants, although microstructures such as grooves can be simultaneously generated integrating the thermally and mechanically stable negative pattern into the mold. The polymer surfaces, for example of PEEK implants, have to be activated to obtain the desired interaction with the biosystem. For bone implants one also needs a nanometer-scale roughness to mimic the apatite crystallites and further nanostructures present in human bone [26].

This study showed that ASC homogenously adhere on oxygen and ammonia plasma treated PEEK substrates, which is a prerequisite for adequate cell differentiation and proliferation, since cytoskeletal tension plays a crucial role in stem cell differentiation [18, 27] and is closely related to the adequate density of focal adhesions, which is associated with the micro- and especially with the nanostructure of the implant's surface. McBeath et al. [27] proved that the cell shape regulates commitment of human mesenchymal stemcells (hMSCs) towards the osteogenic and adipogenic lineage. hMSCs allowed to adhere, flatten, and spread underwent osteogenesis, while unspread, round cells became adipocytes. Kilian et al. [18] verified that when exposed to competing soluble differentiation signals, cells cultured in rectangles with increasing aspect ratio and in shapes with pentagonal symmetry but with different sub-cellular curvature, and with each occupying the same area, display different adipogenesis and osteogenesis profiles. The results reveal that geometric features that increase cytoskeletal tension promote osteogenesis and maybe an approximation to the in vivo characteristics of the microenvironment of the differentiated cells.

To tailor the micro- and nanostructures on the polymer surface, however, is not enough. Surface chemistry is another important parameter, which determines the adsorption of proteins and thus cell behavior. Consequently, it is vital to characterize the net surface charge and the chemical composition of the polymer surface. Both experiments were carefully performed and agree with the expectations. The only exceptions are the presence of fluorine and aluminum. The presence of fluorine is associated with the segregation of moieties from fluorine containing precursors of PEEK. Aluminum probably arises from the vacuum chamber as the result of the high-energetic plasma.

Preparing micro-cantilevers with well-defined nanostructures after chemical activation to measure contractile cell forces as demonstrated by means of Si cantilevers [9] could therefore become an important tool to evaluate the performance of bone implants and to improve their biocompatible properties.

5. CONCLUSIONS

In order to realize load-bearing polymer implants, the mold defining the shape of the implant should be covered with microstructures. These surface structures can be directly replicated into the implant surface in a single step. Hence injection molding allows for easy replication of human tissue topography. In a second processing step, surfaces can be further modified by plasma treatments. This does not only chemically activate the surface, but also creates nanostructures, which can be tailored choosing the process gas composition, the plasma power and the duration of the treatment. One has to consider, however, aging phenomena of the metastable nanostructures and changes owing to contact with water and other species. Stem cell differentiation analysis will support the optimization of the implant surfaces to reach biocompatible properties approximately to that of human tissue itself.

ACKNOWLEDGEMENTS

The authors thank K. Jefimovs (Dübendorf) for the laser micro-machining of the mold, O. Häfeli (Windisch) for the injection molding, A. Caspari (Dresden) for the zeta-potential measurements, S. Adam for the cell-culture work, A. Salamon (Rostock) for methodical support in cell experiment analysis, M. Waser (Muttenz), K. Vogelsang, M. Altana, C. Spreu, S. Stutz, V. Guzenko (Villigen) for their technical assistance. The APTIV™ PEEK films were kindly provided by VICTREX. Financial support was provided by grants from the Swiss Nanoscience Institute (SNI-project 6.2), the Rectors Conference of the Swiss Universities (CRUS), the European Union and the Federal State of Mecklenburg-Vorpommern, Germany (ESF/IV-WM-B34-0006/08).

REFERENCES

[1] J. Park, "Real time measurement of the contactile forces of self organized cardiomyocotes on hybrid biopolymer microcantilevers," Anal. Chem. 77, 6571 (2005).

[2] X. R. Zhang, and X. Xu, "Development of a biosensor based on laser fabricated polymer microcantilevers," Appl. Phys. Lett. 85(12), 2423 (2004).

[3] J. Thaysen, A. D. Yalçinkaya, P. Vettiger *et al.*, "Polymer-based stress sensor with integrated readout," J. Phys. D: Appl. Phys. 35, 2698-2703 (2002).

[4] M. Calleja, M. Nordström, M. Álvarez *et al.*, "Highly sensitive polymer-based cantilever-sensors for DNA detection," Ultramicroscopy 105, 215-222 (2005).

[5] P. Urwyler, O. Häfeli, H. Schift *et al.*, "Disposable polymeric micro-cantilever arrays for sensing," Procedia Eng. 5, 347-350 (2010).

[6] P. Urwyler, J. Köser, H. Schift *et al.*, "Nano-mechanical transduction of polymer micro-cantilevers to detect bio-molecular interactions," Biointerphases 7(1), 8 (2012).

[7] P. Urwyler, H. Schift, J. Gobrecht *et al.*, "Surface patterned polymer micro-cantilever arrays for sensing," Sensors and Actuators A: Physical 172(1), 2-8 (2011).

[8] F. Battiston, J. Ramseyer, H. Lang *et al.*, "A chemical sensor based on a microfabricated cantilever array with simultaneous resonance-frequency and bending readout," Sensors and Actuators B 77, 122-131 (2001).

[9] J. Köser, S. Gaiser, and B. Müller, "Contractile cell forces exerted on rigid substrates," Eur. Cells Mater. 2, 479-487 (2011).

[10] M. Riedel, B. Müller, and E. Wintermantel, "Protein adsorption and monocyte activation on germanium nanopyramids," Biomaterials 22(16), 2307-16 (2001).

[11] B. Müller, "Natural Formation of nanostructures: from fundamentals in metal heteroepitaxy to applications in optics and biomaterials science," Surf. Rev. Lett. 8(1-2), 169-228 (2001).

[12] J. Althaus, C. Padeste, J. Köser *et al.*, "Nanostructuring polyetheretherketone for medical implants," Eur. J. Nanomed. 4, DOI: 10.1515/ejnm-2011-0001 (2012).

[13] C. Chan, T. Ko, and H. Hiraoka, "Polymer surface modification by plasmas and photons," Surf. Sci. Rep. 24, 1-54 (1996).

[14] S. M. Kurtz, and J. N. Devine, "PEEK biomaterials in trauma, orthopedic, and spinal implants," Biomaterials 28, 4845-4869 (2007).

[15] J. Althaus, H. Deyhle, O. Bunk *et al.*, "Anisotropy in polyetheretherketone films," J. Nanophoton. accepted, (2012).

[16] S. W. Ha, R. Hauert, K. H. Ernst *et al.*, "Surface analysis of chemically-etched and plasma-treated polyetheretherketone (PEEK) for biomedical applications," Surf. Coatings Technol. 96, 293-299 (1997).

[17] K. Grundke, H. Jacobatsch, F. Simon *et al.*, "Physico-chemical properties of surface modified polymers," J. Adhesion Sci. Technol. 9, 327-350 (1995).

[18] K. A. Kilian, B. Bugarija, B. T. Lahn *et al.*, "Geometric cues for directing the differentiation of mesenchymal stem cells," Proc. Nat. Acad. Sci. 107(11), 4872-4877 (2010).

[19] K. Peters, Unger, Barth *et al.*, "Induction of apoptosis in human microvascular endothelial cells by divalent cobalt ions. Evidence for integrin-mediated signaling via the cytoskeleton," J. Mater. Sci.: Mater. in Med. 12, 955-958 (2001).

[20] G. Beamson, and D. Briggs, [High resolution XPS of organic polymers—the scienta ESCA 300 data base.] John Wiley & Sons Ltd, Chichester (1992).

[21] D. Clark, B. Cromarty, and A. Dilks, "A theoretical investigation of molecular core binding and relaxation energies in a series of oxygen-containing organic molecules of interest in the study of surface oxidation of polymers,," J. Polymer Sci.: Polymer Chem. 16, 3173-84 (1978).

[22] M. Olla, G. Navarra, B. Elsener *et al.*, "Nondestructive in-depth composition profile of oxy-hydroxide nanolayers on iron surfaces from ARXPS measurement," Surf. Interface Anal. 38(5), 964-974 (2006).

[23] C. Jones and E. Sammann, "The effect of low power plasmas on carbon fibre surfaces," Carbon 28(4), 509-514 (1990).

[24] D. Dohan Ehrenfest, P. Coelho, B. Kang *et al.*, "Classification of osseointegrated implant surfaces: materials, chemistry and topography," Trends Biotechnol. 28(4), 198-206 (2010).

[25] F. Variola, J. B. Brunski, G. Orsini *et al.*, "Nanoscale surface modifications of medically relevant metals: state-of-the art and perspectives," Nanoscale 3(2), 335-353 (2011).

[26] B. Müller, H. Deyhle, D. Bradley *et al.*, "Scanning x-ray scattering: Evaluating the nanostructure of human tissues," Eur. J. Nanomed. 3, 30-33 (2010).

[27] R. McBeath, D. M. Pirone, C. M. Nelson *et al.*, "Cell shape, cytoskeletal tension, and RhoA regulate stem cell lineage commitment," Developmental Cell 6(4), 483-495 (2004).